LIGHTWEIGHT CORN LEAF DISEASE DETECTION MODEL BASED ON YOLOV8N-LSCSBD
/
基于 YOLOv8n-LSCSBD 的轻量化玉米叶病检测模型

Miao XU[1, 2), Xin WU[1), Xuan ZHANG*[2)
[1) College of Information Science and Engineering, Shanxi Agricultural University, Taigu/ China;
[2) College of Agricultural Engineering, Shanxi Agricultural University, Taigu/ China;
Tel: +86 18434764827; E-mail: zhangxuan727@126.com
DOI: https://doi.org/10.35633/inmateh-77-30

Keywords: *corn leaf disease, YOLOv8, Lightweight, Lightweight Shared Convolutional Separable Batch normalization Detection (LSCSBD)*

ABSTRACT
To achieve mobile deployment of corn leaf disease detection, this study proposes a lightweight method, YOLOv8n-LSCSBD. The Lightweight Shared Convolutional Separable Batch normalization Detection (LSCSBD) is used to achieve cross-scale feature sharing convolution and independent normalization, thereby reducing computational complexity and preserving detection accuracy. Comparisons of YOLOv8 training strategies show that using YOLOv8n as the initial model, with a learning rate of 1e-2 and an optimizer of SGD, yields the best performance. Comparisons of different detection head schemes show that YOLOv8n-LSCSBD reduces the model size by 20.6% (to 5.0MB) compared to the original YOLOv8n model. When compared to YOLOv10n and YOLOv11n, the model size decreased by 13.8% and 9.1%, respectively. Notably, YOLOv8n-LSCSBD achieves P of 97.6%, R of 95.4%, mAP@0.5 of 97.7%, and mAP@0.5:0.95 of 87.3%. This method provides an efficient lightweight solution for mobile device deployment.

摘要
为实现玉米叶病的移动端部署检测，本研究提出 YOLOv8n-LSCSBD 轻量化检测方法。该方法通过轻量级共享卷积可分离批量归一化检测头（LSCSBD），实现跨尺度特征共享卷积与独立归一化，在减少计算量的同时保留检测精度。对比 YOLOv8 不同训练策略显示，使用 YOLOv8n 作为初始模型，学习率和优化器分别设置为 1e-2 和 SGD 时性能最佳。对比不同检测头方案显示，使用 LSCSBD 较原始 YOLOv8n 模型大小下降了 20.6%至 5.0MB。与 YOLOv10n 和 YOLOv11n 相比，模型大小分别下降了 13.8%和 9.1%。YOLOv8n-LSCSBD 的 P、R、mAP@0.5 和 mAP@0.5:0.95 分别达到了 97.6%、95.4%、97.7%和 87.3%。该方法为移动端高效部署提供了轻量化解决方案。

INTRODUCTION
As one of the three major food crops in the world (*Farooq et al., 2023; Khaki et al., 2020; Yang et al., 2024*), the yield and quality of corn are directly related to food security and agricultural economic development (*Song et al., 2023; Cui et al., 2023*). According to the Food and Agriculture Organization of the United Nations (FAO), disease outbreaks can lead to a loss ranging from 20% to 40% in maize yield *(FAO, 2020)*. There are many types of corn diseases worldwide that are difficult to detect, among which leaf diseases such as leaf blight disease, gray leaf spot disease, and rust disease are the most common *(Zibanl et al., 2022)*. Traditional disease detection mainly relies on field inspections by agricultural technicians. These inspections are limited by subjective experience, high workload, and environmental conditions, resulting in low detection efficiency, strong time lag, and limited coverage. These issues make it difficult to meet the demands of modern agricultural precision management.

In recent years, breakthroughs in deep learning technology in the field of computer vision have provided a new paradigm for agricultural disease detection *(Shao et al., 2022)*. Sun et al. proposed a multi-scale feature fusion instance detection method based on convolutional neural network (CNN) for detecting maize leaf blight, achieving an mAP of 91.83%, which was about 20% higher than the original SSD algorithm *(Sun et al., 2020)*. Zhang et al. optimized CNN using multiple activation function (MAF) module to detect maize leaf diseases. They employed transfer learning and warm-up methods to accelerate training, improving the accuracy of traditional artificial intelligence methods *(Zhang et al., 2021)*. Chen et al. proposed a lightweight corn disease recognition model, DFCANet (dual fusion block with coordinate attention network), achieving an average recognition accuracy of 98.47% *(Chen et al., 2022)*.

Bi et al. proposed the CD-Mobilenetv3 model to identify maize leaf diseases, replacing the SE module of the original model with the EAC module, and introducing dilated convolution into the model *(Bi et al., 2023)*. The accuracy on open source datasets reached as high as 98.23%. Su et al. improved the YOLOv5 algorithm by adding a CA attention mechanism, replacing the original PANet with BiFPN, and introducing the Focal IoU Loss function *(Su et al., 2023)*. The improved algorithm enhanced performance with only a minimal increase in complexity. Dai et al. proposed a Multi-Task Deep-Learning-Based System for Enhanced Precision Detection and Diagnosis of Corn Leaf Diseases (MTDL-EPDCLD) to enhance the detection and diagnosis of corn leaf disease, and developed a mobile application using the cross platform software development framework Qt *(Dai et al., 2023)*. Song et al. proposed a high-precision detection method based on attention generative adversarial networks (GANs) and few shot learning (*Song et al., 2023*). GANs are used to expand data and generate more training samples. Attention mechanisms are introduced to enable the model to focus more on important parts of the image, thereby improving model performance. Zhang et al. used transfer learning methods to retrain and fine-tune the MoblieNetV2 model on the corn disease dataset, achieving a final test accuracy of 96.83% *(Zhang et al., 2022)*. The optimized corn disease recognition model was applied to application development.

The above studies indicate that object detection models based on deep learning significantly improve the accuracy and efficiency of disease recognition by automatically extracting image features *(Redmon et al., 2018; Ren et al., 2017)*. However, existing models are often designed for laboratory environments and face challenges such as large model size and high computational resource consumption when directly deployed on mobile devices (such as smartphones and drones). This makes it difficult to achieve real-time detection and offline deployment in field scenarios *(Howard et al., 2017)*. Therefore, researching an efficient and accurate lightweight detection model for corn leaf disease adapted to mobile devices has become the key to breaking through the bottlenecks of traditional detection methods and promoting the implementation of smart agriculture.

With fast inference speed, high detection accuracy, and convenient training process, the YOLOv8 model released by Ultralytics becomes a potential foundational model for mobile detection *(Hussain et al., 2023)*. Its efficient inference capability can alleviate the limitations of mobile computing resources, while high accuracy can meet the requirements for precise detection. To further reduce model size and power consumption, this study will conduct lightweight improvements on YOLOv8. The goal is to develop a real-time detection system for corn leaf disease that is compatible with portable intelligent detection devices, thereby providing technical support for the implementation of smart agriculture.

MATERIALS AND METHODS

Dataset construction

In this study, corn leaf disease images from the PlantDoc dataset (*Singh et al., 2020*) were selected as the experimental dataset. The dataset includes 116 images of corn leaf blight, 70 images of corn gray leaf spot, and 114 images of corn rust. Fig. 1 shows sample images of different leaf diseases.

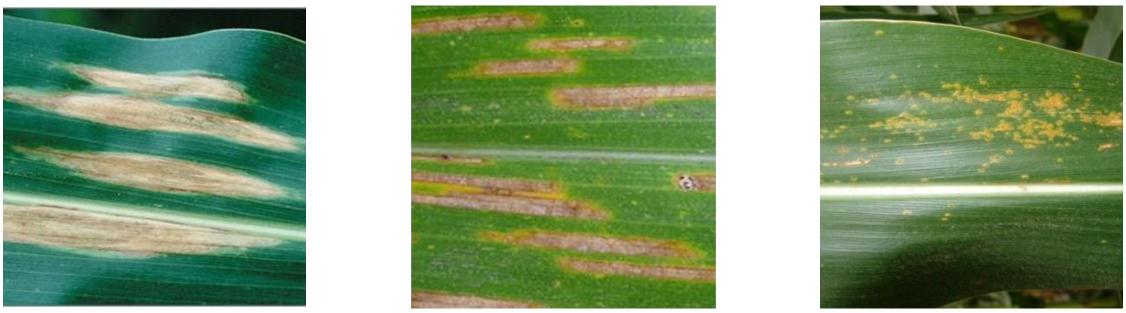

(a) corn leaf blight *(b) corn gray leaf spot* *(c) corn rust*

Fig. 1 - Sample images of different leaf diseases

To address the potential issues of model convergence difficulties and overfitting caused by insufficient training data, various image augmentation techniques (such as scaling and cropping, color tone, saturation, and brightness random adjustments) were employed to expand the corn disease image dataset. The expanded dataset contains 1470 images (486 for leaf blight disease, 500 for gray leaf spot disease, and 484 for rust disease). The dataset was divided into training, validation, and test sets in an 8:1:1 ratio, and the numbers of different disease labels in each dataset are shown in Table 1.

Table 1

Number of annotations of different diseases

Disease	Training set	Validation set	Test set	Total
corn leaf blight	813	71	96	980
corn gray leaf spot	529	56	72	657
corn rust	453	56	50	559
Total	1795	183	218	2196

Improved YOLOv8 Model

Based on the advantages of speed and accuracy of YOLOv8 model, the lightweight version YOLOv8n is chosen as the base model in this paper. To achieve lightweight detection of corn leaf diseases, the Lightweight Shared Convolutional Separable Batch normalization Detection (LSCSBD) is employed to optimize the detection head component.

YOLOv8 model

The YOLOv8 model adopts the classic three-stage structure of "Backbone-Neck-Head" for object detection. The backbone network is responsible for fundamental feature extraction, the neck network performs multi-scale feature fusion, and the detection head performs object detection based on the fused features. Fig. 2 shows the architecture of the YOLOv8 model.

Input: Denotes the input RGB images with a fixed resolution of 640×640 pixels.

ConvModule: Represents a convolutional module consisting of 2D convolution, batch normalization, and SiLU activation, responsible for basic feature transformation and nonlinear enhancement.

C2f: Refers to the improved C3 module with enhanced gradient flow; it splits feature maps into two branches for partial fusion, balancing computational efficiency and feature integrity.

SPFF: Stands for Spatial Pyramid Feature Fusion, a multi-scale pooling module that aggregates contextual information to capture objects of different sizes.

PAN-FPN: Indicates the hybrid feature fusion architecture combining Path Aggregation Network (PAN) and Feature Pyramid Network (FPN), enabling bidirectional feature transmission.

Detect: Denotes the detection head module in the model, which is responsible for outputting final detection results (including object categories, bounding box coordinates, and objectness scores).

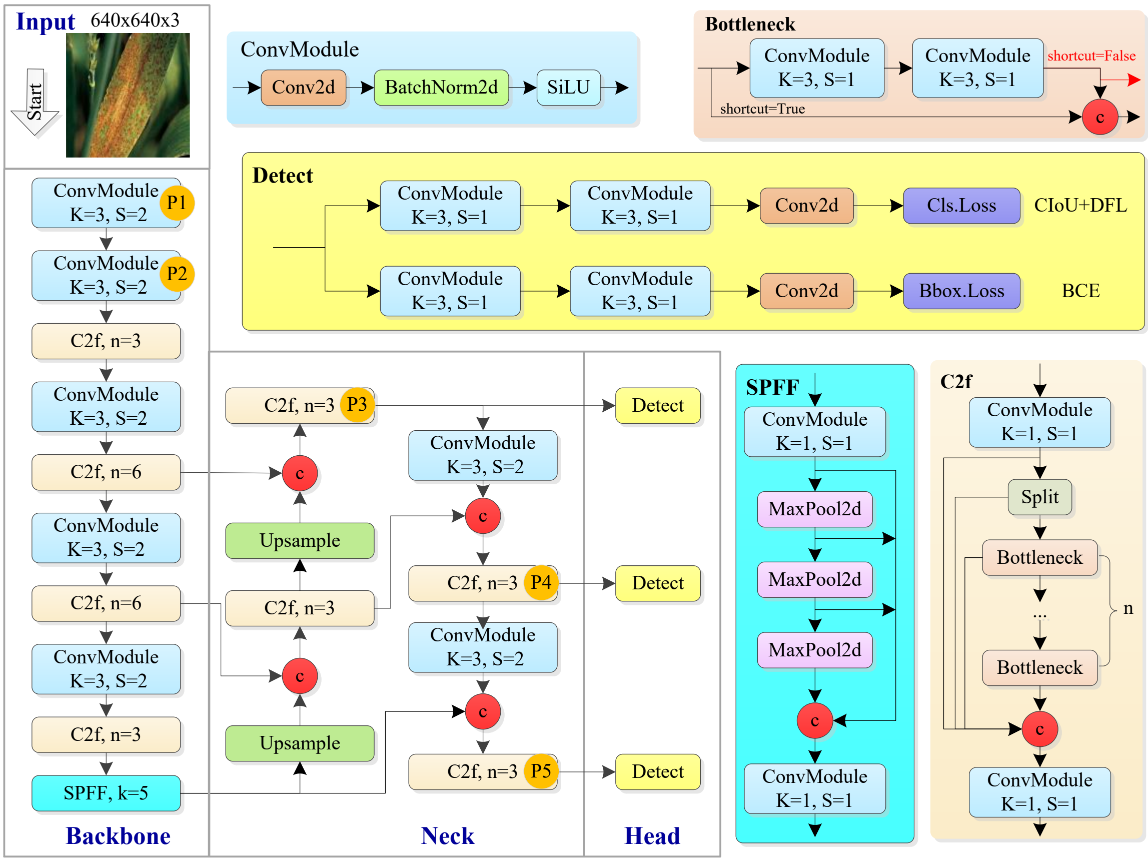

Fig. 2 - YOLOv8 network structure

The key design of YOLOv8 model includes:

(1) Backbone: Based on the CSP (Cross Stage Partial) concept, ConvModule, C2f, and SPFF modules are integrated to improve feature extraction efficiency while ensuring stability.

(2) Neck: Drawing on the PAN-FPN architecture, the convolution in the upsampling stage is simplified, and C2f is used, optimizing the feature fusion process.

(3) Head: The Detect module adopts a decoupled head structure to separate classification and detection tasks, effectively capturing multi-scale targets and improving detection accuracy.

Detect_LSCSBD

The detection head is a core component of the model, responsible for predicting the class and location information of targets from feature maps. The YOLOv8 detection head adopts an anchor-free design, reducing the computational load associated with anchor generation and enhancing the detection ability for targets of different shapes and sizes. As shown in Fig. 2, the neck network performs multi-scale feature fusion, extracting information from P3, P4, and P5 feature layers to generate multi-scale feature maps for multi-scale target detection by the detection head. Additionally, the classification and regression tasks are decoupled in the detection head, employing Binary Cross-Entropy (BCE) loss for classification and Complete Intersection over Union (CIoU) loss for regression, combined with task alignment matching strategies to further optimize detection performance.

Although the YOLOv8 detection head performs well, its computational load and complexity constrain real-time deployment. To address this, the LSCSBD is used to improve the detection head, called Detect_LSCSBD. As shown in Fig.3, the key design of the detection head is as follows:

(1) Multi-scale feature preprocessing: For the P3/P4/P5 multi-scale features output by the neck network, Detect_LSCSBD employs independent 1x1 convolution to achieve channel dimensionality reduction and feature calibration. This design preserves the independence of features at each scale, thereby avoiding the loss of small target information caused by direct mixing of cross scale features.

(2) Shared Convolution and Normalization: Detect_LSCSBD uses two sets of shared 3×3 convolution kernels to process multi-scale features, significantly reducing the number of parameters through parameter reuse and forcing cross-scale feature learning of universal patterns. Each scale is equipped with an independent normalization layer to ensure that the distributions of features at different scales are calibrated separately, ensuring training stability.

(3) Task decoupling and scale adaptation: Classification and regression tasks are decoupled through independent branches, reducing mutual interference. For the different receptive field characteristics of P3/P4/P5, independent scale adjustment modules (Scale) are designed to ensure adaptability for detecting objects of different sizes.

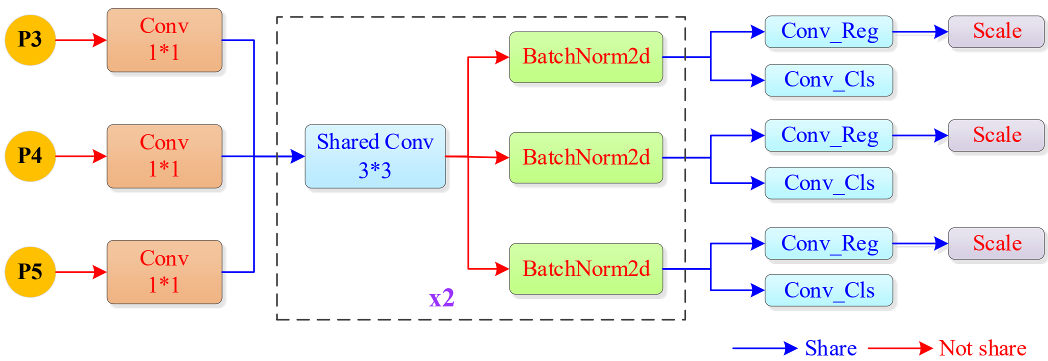

Fig. 3 - Detect_LSCSBD Structure

Experimental Platform and Network Parameter Settings

This study was conducted on the Windows 11 operating system. The hardware configuration includes an Intel Core i5 processor, 16GB of RAM, and an NVIDIA GeForce RTX3050Ti GPU. The programming language used is Python 3.12.7, with PyCharm serving as the integrated development environment (IDE) for Python. The deep learning framework employed is PyTorch with CUDA version 12.4.

The key training parameters for the experiments are set as follows: input image size is uniformly scaled to 640 × 640 pixels. The number of training epochs is set to 200. The range for random scaling augmentation of images is set to 0.9 (i.e. the image size is randomly adjusted within a range of 0.9 times the original size). The application probability of mosaic data augmentation strategy is set to 100%.

Model evaluation metrics

To evaluate the performance of the model, several metrics are employed, including *Precision (P)*, *Recall (R)*, *P-R* curve, *mean Average Precision (mAP)*, and model size. *Precision (P)* measures the accuracy of model predictions, and a high precision means that the model has fewer false positives when predicting targets. The calculation formula is shown in equation (1):

$$P = \frac{TP}{TP + FP} \tag{1}$$

where: *TP (True Positive)* represents the number of correctly predicted positive samples, and *FP (False Positive)* represents the number of incorrectly predicted positive samples.

Recall (R) measures the completeness of the model's targets detection, and a high recall means that the model can discover as many targets as possible, reducing false negatives. The calculation formula is shown in equation (2):

$$R = \frac{TP}{TP + FN} \tag{2}$$

where: *FN (False Negative)* represents the number of positive samples incorrectly predicted as negative.

The *P-R* curve is constructed by plotting *P* values against their corresponding *R* values across different decision thresholds, directly reflecting the dynamic trade-off between the two metrics.

The *mAP* comprehensively considers the average detection accuracy of the model across multiple classes. For each class, *Average Precision (AP)* is computed as the area under the *P-R* curve, and *mAP* is the mean of *AP* values across all classes, serving as a core metric for overall performance in object detection. Model size refers to the storage space required by the detection model (usually measured in MB). A smaller model can be adapted to devices with limited resources, thereby reducing hardware costs and improving real-time performance, which meets the requirements of lightweight deployment.

RESULTS

Comparative analysis of training strategies

Learning rate, optimizer, and pre-trained weights are core parameters in the training process, directly influencing the convergence speed, detection accuracy, and generalization ability of the model. This experiment conducts comparative analysis from these three dimensions to provide a basis for parameter selection and model optimization.

Performance analysis of different learning rates

The learning rate plays a crucial regulatory role in balancing model lightweight process and high accuracy, and its impact on model convergence stability and high precision is fully tested. To analyze the performance differences of YOLOv8 under different learning rates, the Stochastic Gradient Descent (SGD) algorithm was chosen as the optimizer, with learning rates set to 1e-4, 1e-3, 1e-2, and 1e-1, respectively.

As shown in Table 2, when the learning rate was 1e-4, underfitting was caused by slow updates, resulting in an mAP@0.5:0.95 of only 0.712. Conversely, when the learning rate was 1e-1, instability was caused by a large step size, yielding an mAP@0.5:0.95 of only 0.755. The performance was similar for learning rates of 1e-3 and 1e-2, but the overall performance at 1e-2 was superior to that at 1e-3. Therefore, a learning rate of 1e-2 was used for subsequent training in this experiment.

Table 2

Detection results of different learning rates

Learning rate	Categories	P	R	mAP@0.5	mAP@0.5:0.95
1e-4	Corn leaf blight	0.82	0.69	0.829	0.571
	Corn gray leaf spot	0.954	0.746	0.883	0.769
	Corn rust leaf	0.919	0.87	0.917	0.794
	all	**0.898**	**0.769**	**0.876**	**0.712**
1e-3	Corn leaf blight	0.918	0.893	0.939	0.781
	Corn gray leaf spot	0.983	0.935	0.971	0.891
	Corn rust leaf	0.962	0.942	0.981	0.89
	all	**0.954**	**0.924**	**0.964**	**0.854**
1e-2	Corn leaf blight	0.928	0.921	0.961	0.802
	Corn gray leaf spot	1	0.965	0.979	0.914
	Corn rust leaf	0.981	0.981	0.991	0.905
	all	**0.97**	**0.956**	**0.977**	**0.874**

Learning rate	Categories	P	R	mAP@0.5	mAP@0.5:0.95
1e-1	Corn leaf blight	0.847	0.759	0.834	0.612
	Corn gray leaf spot	0.944	0.841	0.937	0.807
	Corn rust leaf	0.975	0.889	0.964	0.846
	all	**0.922**	**0.83**	**0.912**	**0.755**

Performance analysis of different optimizers

Different optimizers use different algorithms to update model parameters, which have a significant impact on model performance. The experiment compared SGD, AdamW, and NAdam.

As shown in Table 3, in the corn leaf disease detection experiment (dataset: corn leaf disease images from PlantDoc, fixed hyperparameters:1e-2 learning rate), the SGD optimizer demonstrated significantly superior performance across all metrics compared to AdamW and NAdam. It particularly exhibited strong data fitting capabilities and efficient convergence across various categories during detection. Therefore, the SGD optimizer was used for subsequent training in this experiment.

Table 3

Detection results of different optimizers

Optimizer	Categories	P	R	mAP@0.5	mAP@0.5:0.95
AdamW	Corn leaf blight	0.868	0.857	0.904	0.689
	Corn gray leaf spot	0.949	0.887	0.958	0.827
	Corn rust leaf	0.919	0.907	0.949	0.867
	all	**0.912**	**0.884**	**0.937**	**0.795**
NAdam	Corn leaf blight	0.859	0.786	0.87	0.663
	Corn gray leaf spot	0.964	0.847	0.939	0.797
	Corn rust leaf	0.956	0.907	0.954	0.846
	all	**0.927**	**0.847**	**0.921**	**0.768**
SGD	Corn leaf blight	0.928	0.921	0.961	0.802
	Corn gray leaf spot	1	0.965	0.979	0.914
	Corn rust leaf	0.981	0.981	0.991	0.905
	all	**0.97**	**0.956**	**0.977**	**0.874**

Performance analysis of different pre-trained weight models

To evaluate the effect of various pre-trained weights on the transfer learning performance of YOLOv8 model, the variants of YOLOv8 (n/s/m/l/x) were used for comparative experiments. The variants of YOLOv8 belong to the same generation of iterative designs (not multi-generation iterations) and have a "scaled-up" relationship. This scaling is achieved by adjusting the network's depth (number of layers) and width (number of feature channels), while the core architecture remains unchanged. They mainly differ in model scale, computational cost, and detection performance.

As shown in Table 4, the P, R, mAP@0.5, and mAP@0.5:0.95 of YOLOv8n achieved 0.97, 0.956, 0.977, and 0.874, respectively. YOLOv8n demonstrated significantly superior performance metrics across both individual categories and overall results compared to the s \ m \ l \ x, demonstrating a good balance between lightweight and high precision. Therefore, YOLOv8n is the optimal pre-trained weight model for this experimental dataset.

Table 4

Detection results of different pre-trained weight models

Model	Categories	P	R	mAP@0.5	mAP@0.5:0.95
YOLOv8n	Corn leaf blight	0.928	0.921	0.961	0.802
	Corn gray leaf spot	1	0.965	0.979	0.914
	Corn rust leaf	0.981	0.981	0.991	0.905
	all	**0.97**	**0.956**	**0.977**	**0.874**
YOLOv8s	Corn leaf blight	0.888	0.777	0.867	0.652
	Corn gray leaf spot	0.91	0.889	0.945	0.826
	Corn rust leaf	0.936	0.926	0.973	0.874
	all	**0.911**	**0.864**	**0.929**	**0.784**
YOLOv8m	Corn leaf blight	0.902	0.768	0.878	0.67
	Corn gray leaf spot	0.949	0.886	0.957	0.843
	Corn rust leaf	0.943	0.926	0.967	0.855
	all	**0.931**	**0.86**	**0.934**	**0.789**

Model	Categories	P	R	mAP@0.5	mAP@0.5:0.95
YOLOv8l	Corn leaf blight	0.802	0.786	0.818	0.599
	Corn gray leaf spot	0.919	0.896	0.956	0.816
	Corn rust leaf	0.964	0.889	0.943	0.837
	all	**0.895**	**0.857**	**0.906**	**0.751**
YOLOv8x	Corn leaf blight	0.918	0.741	0.874	0.649
	Corn gray leaf spot	0.973	0.841	0.958	0.858
	Corn rust leaf	0.976	0.926	0.962	0.849
	all	**0.956**	**0.836**	**0.931**	**0.786**

Comparative analysis of different detection heads

By adjusting the detection head in terms of its structure design, feature utilization, and computational efficiency, model size can be compressed using lightweight techniques while maintaining accuracy. This project compared the performance of RSCD, LSCD, and LSCSBD detection head optimization models.

As indicated in Table 5, the RSCD, LSCD, and LSCSBD models were each smaller than the original YOLOv8 model by 17.5%, 20.6%, and 20.6% respectively. The model using RSCD detection head showed decreases in P, R mAP@0.5 and mAP@0.5 0.95. The model using LSCD detection head showed decreases in R, mAP@0.5, and mAP@0.5:0.95. The model with LSCSBD reduced the model size by 20.6% (to 5.0 MB), with performance metrics comparable to those of YOLOv8, making it the optimal solution balancing “lightweight” and “high accuracy”.

Table 5

Detection results of different detection heads

Detection head	Categories	P	R	mAP@0.5	mAP@0.5:0.95	Model size/MB
Original	Corn leaf blight	0.928	0.921	0.961	0.802	6.3
	Corn gray leaf spot	1	0.965	0.979	0.914	
	Corn rust leaf	0.981	0.981	0.991	0.905	
	all	**0.97**	**0.956**	**0.977**	**0.874**	
RSCD	Corn leaf blight	0.962	0.895	0.954	0.799	5.2
	Corn gray leaf spot	0.967	0.968	0.968	0.9	
	Corn rust leaf	0.948	0.981	0.989	0.89	
	all	**0.959**	**0.948**	**0.97**	**0.863**	
LSCD	Corn leaf blight	0.947	0.902	0.936	0.781	5.0
	Corn gray leaf spot	0.993	0.968	0.985	0.928	
	Corn rust leaf	0.981	0.977	0.987	0.904	
	all	**0.974**	**0.949**	**0.969**	**0.871**	
LSCSBD	Corn leaf blight	0.945	0.938	0.961	0.799	5.0
	Corn gray leaf spot	0.984	0.946	0.982	0.928	
	Corn rust leaf	1	0.978	0.99	0.891	
	all	**0.976**	**0.954**	**0.977**	**0.873**	

To better evaluate the performance of detection models, the results of optimizing models for different detection heads were visualized. As shown in Fig. 4, different detection heads can effectively identify different leaf diseases, and LSCSBD has better detection accuracy than RSCD and LSCD.

Original Image

YOLOv8n

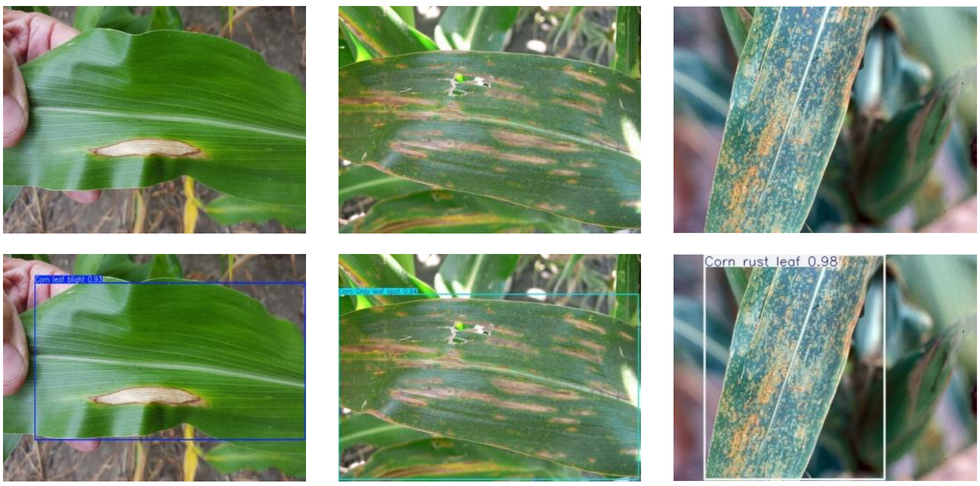

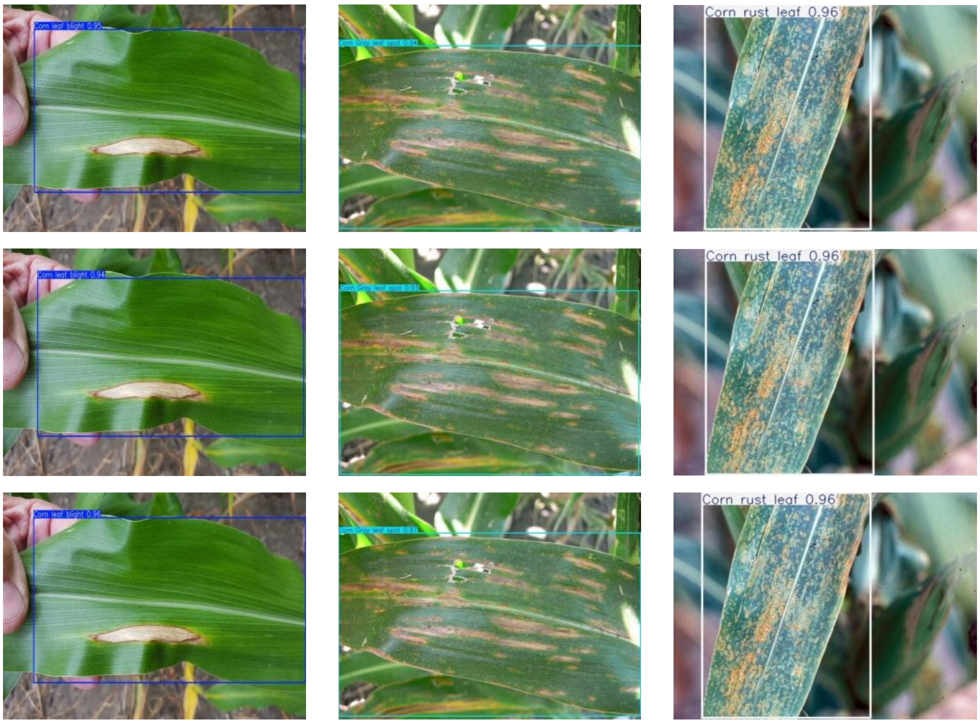

YOLOv8n-RSCD

YOLOv8n-LSCD

YOLOv8n-LSCSBD

(a) corn leaf blight (b) corn gray leaf spot (c) corn rust

Fig. 4 - Visual comparison of different detection heads

Comparative analysis of different network models

The YOLO series models continue to iterate in the field of object detection, and different versions have been optimized in terms of accuracy, speed, and model size. To compare the effectiveness of the improved model more clearly, the performance of YOLOv8n, YOLOv10n, YOLOv11n, and YOLOv8n-LSCSBD were compared.

As shown in Table 6, the YOLOv8n-LSCSBD model performs best in all performance metrics. The model size of YOLOv8n-LSCSBD decreased by 20.6%, 13.8%, and 9.1% compared to YOLOv8n, YOLOv10n, and YOLOv11n, respectively.

Table 6

Detection results of different models

Model	Categories	P	R	mAP@0.5	mAP@0.5:0.95	Model size/MB
YOLOv8n	Corn leaf blight	0.82	0.69	0.829	0.571	6.3
	Corn gray leaf spot	0.954	0.746	0.883	0.769	
	Corn rust leaf	0.919	0.87	0.917	0.794	
	all	**0.898**	**0.769**	**0.876**	**0.712**	
YOLOv10n	Corn leaf blight	0.807	0.485	0.679	0.497	5.8
	Corn gray leaf spot	0.864	0.714	0.827	0.725	
	Corn rust leaf	0.795	0.815	0.871	0.779	
	all	**0.822**	**0.671**	**0.792**	**0.667**	
YOLOv11n	Corn leaf blight	0.866	0.69	0.814	0.567	5.5
	Corn gray leaf spot	0.965	0.794	0.914	0.784	
	Corn rust leaf	0.934	0.87	0.924	0.809	
	all	**0.922**	**0.785**	**0.884**	**0.72**	
YOLOv8n-LSCSBD	Corn leaf blight	0.945	0.938	0.961	0.799	5.0
	Corn gray leaf spot	0.984	0.946	0.982	0.928	
	Corn rust leaf	1	0.978	0.99	0.891	
	all	**0.976**	**0.954**	**0.977**	**0.873**	

To better evaluate the performance of detection models, the results of different models were visualized. As shown in Fig. 5, YOLOv8n-LSCSBD has a good detection effect on different leaf diseases.

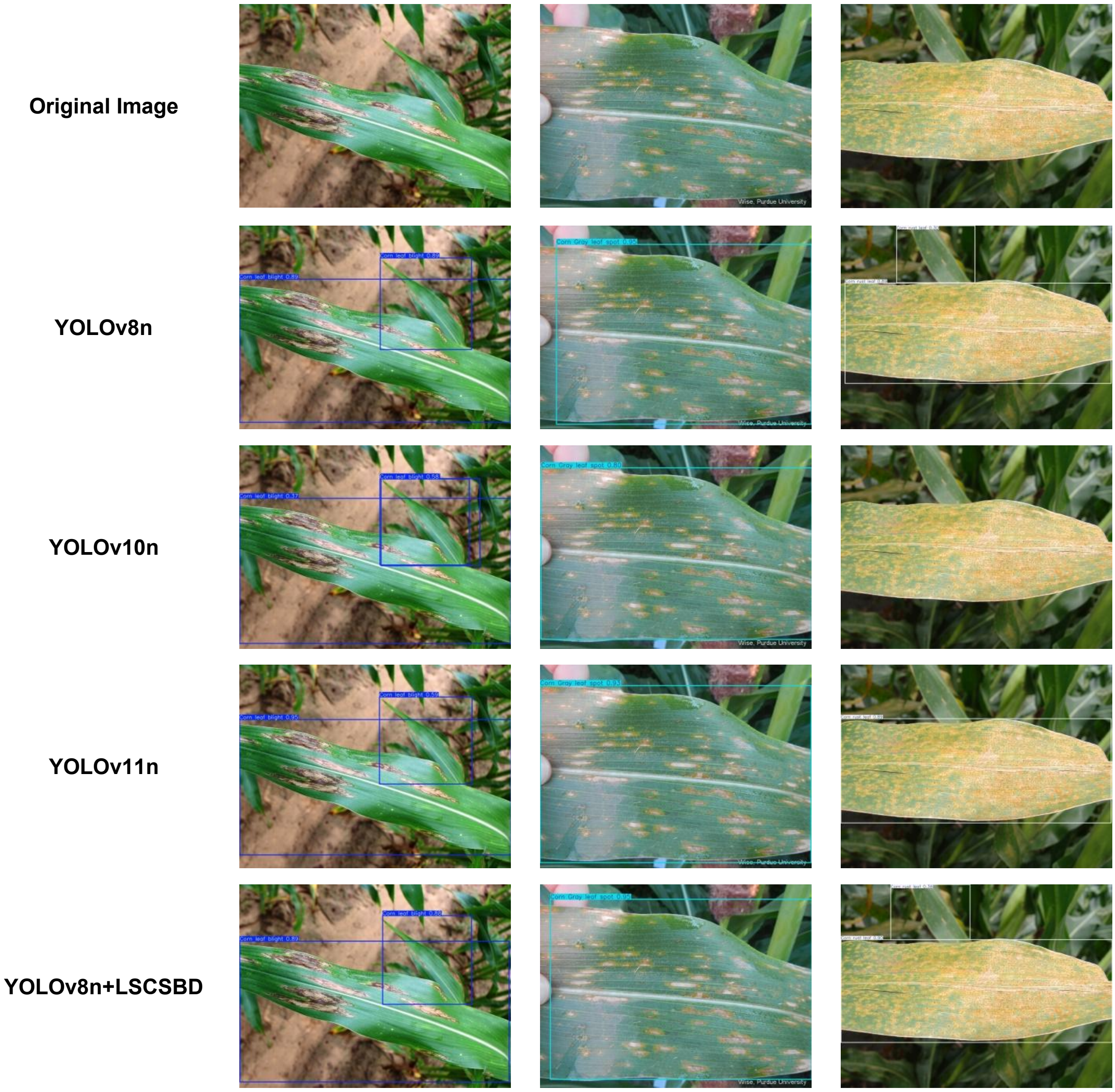

(a) corn leaf blight (b) corn gray leaf spot (c) corn rust

Fig. 5 - Visual comparison of different models

CONCLUSIONS

(1) A lightweight detection model YOLOv8n-LSCSBD was proposed. This design utilizes cross scale shared convolution parameter reuse, independent normalization layer calibration, and task decoupling to reduce computational and parameter complexity while maintaining detection accuracy and improving real-time deployment efficiency.

(2) By comparing different learning rates (1e-4, 1e-3, 1e-2, 1e-1), optimizers (SGD, AdamW, NAdam), and pre training weights (YOLOv8n, s, m, l, x), the optimal training strategy was determined. The optimal combination was identified as a learning rate of 1e-2, optimizer of SGD, and pre-trained weight of YOLOv8n, which improved mAP@0.5 0.95 by 1.8% compared to the default configuration.

(3) Comparisons among different detection head schemes showed that the LSCSBD model reduced the model size to 5.0 MB. Furthermore, the performance metrics of YOLOv8n-LSCSBD were on par with the original YOLOv8.

Compared to YOLOv8n, YOLOv10n, and YOLOv11n, the YOLOv8n-LSCSBD model achieved size reductions of 20.6%, 13.8%, and 9.1%, respectively, while its mAP@0.5:0.95 improved by 16.1, 20.6, and 15.3 percentage points, respectively. This validates the comprehensive advantages of the lightweight design in accuracy and efficiency.

ACKNOWLEDGEMENT

This research, titled “Lightweight corn leaf disease detection model based on YOLOv8n-LSCSBD”, was funded by the College Students Innovation Training Program of Shanxi Agricultural University (Intelligent Detection System for Corn Leaf Disease Based on Deep Learning, S202510113058).

REFERENCES

[1] Bi, C.G.; Xu, S.Z.; Hu, N.; Zhang, S.; Zhu, Z.Y.; Yu, H.L. (2023), Identification method of corn leaf disease based on improved Mobilenetv3 model [J]. *Agronomy*, 13(2): 300.

[2] Chen, Y.; Chen, X.; Lin, J.; Pan, R.; Cao, T.; Cai, J.; Yu, D.; Cernava, T.; Zhang, X. (2022), DFCANet: A Novel Lightweight Convolutional Neural Net-work Model for Corn Disease Identification [J]. *Agriculture*, 12, 2047.

[3] Cui, S; Su, Y.L.; Duan, K.; Liu, Y. (2023), Maize leaf disease classification using CBAM and lightweight Autoencoder network [J]. *Journal of ambient intelligence and humanized computing*, 14(6): 7297-7307.

[4] Dai, D.; Xia, P.; Zhu, Z.; Che, H. (2023), MTDL-EPDCLD: A Multi-Task Deep-Learning-Based System for Enhanced Precision Detection and Diagnosis of Corn Leaf Diseases [J]. *Plants*, 12(13), 2433.

[5] Farooq, A.; Farooq, N.; Akbar, H.; Hassan, Z.U.; Gheewala, S.H. (2023), A Critical Review of Climate Change Impact at a Global Scale on Cereal Crop Production [J], *Agronomy*, 13(1):162.

[6] Food and Agriculture Organization of the United Nations (FAO). (2020), *Global Crop Prospects and Food Security Report*. Rome: FAO.

[7] Howard, A.G.; Zhu, M.; Chen, B.; Kalenichenko, D.; Wang, W.; Weyand, T. (2017), MobileNets: Efficient Convolutional Neural Networks for Mobile Vision Applications. *arXiv preprint* arXiv:1704.04861.

[8] Hussain, M. (2023), YOLO-v1 to YOLO-v8, the Rise of YOLO and Its Complementary Nature toward Digital Manufacturing and Industrial Defect Detection [J]. *Machines*, 11(7): 677.

[9] Khaki, S.; Pham, H.; Han, Y.; Kuhl, A.; Kent, W.; Wang, L. (2020), Convolutional Neural Networks for Image-Based Maize kernel Detection and Counting [J]. *Sensors*, 20(9):2721.

[10] Redmon, J., Farhadi, A. (2018), YOLOv3: An Incremental Improvement. *arXiv preprint* arXiv:1804.02767.

[11] Ren, S.; He, K.; Girshick, R.; Sun, J. (2017), Faster R-CNN: Towards Real-Time Object Detection with Region Proposal Networks [J]. *IEEE Transactions on Pattern Analysis and Machine Intelligence*, 39(6):1137-1149.

[12] Shao, M.Y; Zhang, J.H.; Feng, Q.; Chai, X.J.; Zhang, N.; Zhang, W.R. (2022), Research Progress of Deep Learning in Detection and Recognition of Plant Leaf Diseases (深度学习在植物叶部病害检测与识别的研究进展) [J]. *Smart Agriculture*, 4(01):29-46.

[13] Singh, D.; Jain, N.; Jain, P.; Kayal, P.; Kumawat, S.; Batra, N. (2020), PlantDoc: A dataset for visual plant disease detection [C]. *In Proceedings of the 7th ACM IKDD CoDS and 25th COMAD on Goa*, Hyderabad, India, 5–7 January, 249–253.

[14] Song, Y.H.; Zhang, H.Y.; Li, J.Q.; Ye, R.; Zhou, X.C.; Dong, B.W.; Fan, D.C.; Li, L.. (2023), High-Accuracy Maize Disease Detection Based on Attention Generative Adversarial Network and Few-Shot Learning [J]. *Plants*, 12(17).

[15] Su, J.K.; Duan, X.H.; Ye, Z.B. (2023), Research on Corn Disease Detection Based on Improved YOLOv5 Algorithm (改进 YOLOv5 算法的玉米病害检测研究) [J], *Journal of Frontiers of Computer Science and Technology*, 17(4): 933-941.

[16] Sun, J.; Yang, Y.; He, X.; Wu, X. (2020), Northern maize leaf blight detection under complex field environment based on deep learning [J]. *IEEE Access*, 8:33679-33688.

[17] Yang, Z.; Fang, S.; Huang, H. (2024), Maize leaf disease image enhancement algorithm using TFEGAN [J]. *Crop Protection, 182*(000), 12.

[18] Zhang, Y.T.; Su, Q.M. (2023), Image Recognition of Corn Disease Based on Transfer Learning (基于迁移学习的玉米病害图像识别) [J]. *Journal of Agricultural Science and Technology*, 25(10):119-125.

[19] Zhang, Y.; Wa, S.; Liu, Y.; Zhou, X.; Sun, P.; Ma, Q. (2021), High-Accuracy Detection of Maize Leaf Diseases CNN Based on Multi-Pathway Activation Function Module [J]. *Remote Sens*, 13, 4218.

[20] Zibani, A.; Ali, S.; Benslimane, H. (2022), Corn diseases in Algeria: first report of three Bipolaris and two Exserohilum species causing leaf spot and leaf blight diseases [J]. *Cereal Research Communications*, 50(3): 449-461.